



**HAL**  
open science

# Analytical and numerical study of Soret mixed convection in two sided lid-driven horizontal cavity: optimal species separation

Abdelkader Mojtabi, Ali Khouzam, Loujaine Yacine, Marie-Catherine Charrier-Mojtabi

## ► To cite this version:

Abdelkader Mojtabi, Ali Khouzam, Loujaine Yacine, Marie-Catherine Charrier-Mojtabi. Analytical and numerical study of Soret mixed convection in two sided lid-driven horizontal cavity: optimal species separation. *International Journal of Heat and Mass Transfer*, 2019, 139, pp.1037-1046. 10.1016/j.ijheatmasstransfer.2019.05.074 . hal-02152279

**HAL Id: hal-02152279**

**<https://hal.science/hal-02152279>**

Submitted on 11 Jun 2019

**HAL** is a multi-disciplinary open access archive for the deposit and dissemination of scientific research documents, whether they are published or not. The documents may come from teaching and research institutions in France or abroad, or from public or private research centers.

L'archive ouverte pluridisciplinaire **HAL**, est destinée au dépôt et à la diffusion de documents scientifiques de niveau recherche, publiés ou non, émanant des établissements d'enseignement et de recherche français ou étrangers, des laboratoires publics ou privés.





## Open Archive Toulouse Archive Ouverte (OATAO)

OATAO is an open access repository that collects the work of Toulouse researchers and makes it freely available over the web where possible

This is an author's version published in: <http://oatao.univ-toulouse.fr/23946>

**Official URL:** <https://doi.org/10.1016/j.ijheatmasstransfer.2019.05.074>

### To cite this version:

Mojtabi, Abdelkader  and Khouzam, Ali and Yacine, Loujaine and Charrier-Mojtabi, Marie-Catherine  *Analytical and numerical study of Soret mixed convection in two sided lid-driven horizontal cavity: optimal species separation.* (2019) *International Journal of Heat and Mass Transfer*, 139. 1037-1046. ISSN 0017-9310

Any correspondence concerning this service should be sent to the repository administrator: [tech-oatao@listes-diff.inp-toulouse.fr](mailto:tech-oatao@listes-diff.inp-toulouse.fr)

## **Analytical and numerical study of Soret mixed convection in two sided lid-driven horizontal cavity: optimal species separation**

Abdelkader Mojtabi<sup>1</sup>, Ali Khouzam<sup>2</sup>, Loujaine Yacine<sup>3</sup>, Marie-Catherine Charrier Mojtabi<sup>1</sup>

<sup>1</sup> *Université de Toulouse; IMFT (Institut de Mécanique des Fluides de Toulouse); Allée du Professeur Camille Soula, F-31400 Toulouse, France*

<sup>2</sup> *Icam, Institut Catholique d'Arts et Métiers, site de Paris-Sénart - 34 Points de Vue, 77127 Lieusaint, France*

<sup>3</sup> *ENSIM- École Nationale Supérieure d'Ingénieurs du Mans, 1 Rue Aristote, 72000 Le Mans, France*

## Abstract

The coupling between shear-driven convection and thermo-diffusion is a complex phenomenon due to the interactions between the different forces inside the fluid mixture. This paper studies the species separation that may appear in a parallelepipedic cell filled by a binary mixture. Dirichlet boundary conditions are imposed with differentially heated horizontal walls. Each wall can be animated with a uniform velocity. More precisely, two velocities  $U_p \vec{e}_x$  and  $f U_p \vec{e}_x$  are applied at the upper and the lower horizontal walls respectively. An analytical solution, based on the parallel flow approximation in the core region of the cavity of large aspect ratio, is obtained as a function of the dimensionless parameters of the problem. The species separation is optimized according to the multiple control parameters of the problem. The velocity field obtained is the superposition of the flow generated by the velocity of the walls under weightless conditions and thermoconvective flow under gravity only. The combination of these two flows leads to a mixed convection flow with a single convective cell for  $f \in [-1, 0]$  and two superposed cells for  $f \in [0, 1]$ . Only unicellular flow leads to a notable species separation. This study shows that the effective species separation admits a partial optimum as a function of  $f$  and  $U_p$ . As in the case of thermogravitational columns, there is no optimum species separation with respect to parameters  $\Delta T$  and  $H$  but, for a fixed temperature difference  $\Delta T$ , there is a thickness  $H$  that optimizes the separation and vice versa. 2D and 3D direct numerical simulations are performed using a finite element method in order to corroborate the analytical results. The influence of mass Péclet number on the diffusive relaxation time is determined numerically. Taking into account the confinement of the medium in the third dimension, perpendicular to a vertical plane, we show that the aspect ratio in the y-direction has an influence on the species separation.

**Keywords:** *Soret effect; thermodiffusion; mixed Convection; species separation, thermogravitation*

Nomenclature			
$A$	Aspect ratio of the cavity $L/H$	$S$	Non-dimensional species separation ( $S = mA$ ) Soret number, $D_T/D$ , [ $K^{-1}$ ]
$A_y$	Aspect ratio of the cavity $l/H$	$S^*$	Dimensional species separation ( $S^* = m^*L$ )
$a$	Thermal diffusivity, [ $m^2 s^{-1}$ ]	$t$	Dimensionless time

$C$	Modified mass fraction $(C^* - C_0^*)/\Delta C$	$T$	Dimensionless temperature
$C_0^*$	Initial mass fraction	$T_0^*$	Reference temperature
$D$	Mass diffusion coefficient	$U_p$	Wall velocity [m/s]
$D_T$	Thermodiffusion coefficient [ $m^2s^{-1}K^{-1}$ ]	$(u, v)$	Dimensionless velocity components in ( $x, z$ ) directions
$f$	Velocity Ratio of moving walls	<i>Greek symbols</i>	
$g$	Gravitational acceleration [ $ms^{-2}$ ]	$\beta_C$	Solutal expansion coefficient
$H$	Height of the enclosure [m]	$\beta_T$	Thermal expansion coefficient [1/K]
$L$	Length of the enclosure [m]	$\lambda$	Thermal conductivity [ $Wm^{-1}K^{-1}$ ]
$m$	Mass fraction gradient	$\mu$	Dynamic viscosity [Pa.s]
$Le$	Lewis number	$\nu$	Kinematic viscosity of the mixture, [ $m^2s^{-1}$ ]
$P$	Pressure [Pa]	$\rho$	Density of the mixture, [ $kgm^{-3}$ ]
$Pe$	Péclet number	$\psi$	Separation ratio factor
$Pe_m = PeLe$	Mass Péclet number	<i>Subscripts</i>	
$Pr$	Prandtl number,	0	Reference state
$Ra$	Rayleigh number	*	Dimensional variables
$Ra_m = Ra\psi Le$	Mass Rayleigh number	p	Index for the wall

## 1. Introduction

The coupling between buoyancy forces due to a temperature gradient, imposed on a fluid layer heated from below, and forced convection due to shear stress leads to the well-known phenomenon called mixed convection. Mixed convection has been studied by several authors because applications of practical interest can be found for it in many industrial processes [1]. Experimental studies and direct numerical simulations have shown that mixed convection with combined driving forces depends on two control parameters: the Rayleigh and the Péclet numbers. Flow visualizations performed in a lid-driven cavity, have led to a better understanding of the underlying physical mechanisms [2].

In binary fluid mixtures subjected to temperature gradient, a mass fraction gradient appears due to the thermodiffusion or Soret effect. In addition to the usual expression for the mass flux  $\vec{J}_m$  given by Fick's law, a part due to the temperature gradient is added such that:

$$\vec{J}_m = -\rho D \nabla C^* - \rho D_T C^* (1 - C^*) \nabla T^*$$

where  $D$  is the mass diffusion coefficient,  $D_T$  the thermodiffusion coefficient,  $\rho$  the mixture density,  $T^*$  the temperature and  $C^*$  the mass fraction of the constituent of interest. In many studies, the authors consider that  $C^*(1 - C^*) \approx C_0^*(1 - C_0^*)$  where  $C_0^*$  is the initial mass fraction.

Many works concerning Soret-driven convection in binary mixtures have been published in the last two decades and many fundamental and industrial applications have been found, such as the study of contaminants in saturated soil, drying processes or solute transfer in the mushy layer during the solidification of binary alloys.

Charrier-Mojtabi et al. [3] developed a linear stability analysis of the unicellular flow that appears at the onset of convection in a horizontal porous cavity saturated by a binary fluid and heated from below. These authors showed that, if the separation ratio,  $\psi$ , was positive and greater than a particular value,  $\psi_{uni}$ , it was possible to separate the species of a binary fluid mixture between the two ends of the horizontal cell.

Mialdun et al. [4] made measurements of diffusion, thermodiffusion and Soret coefficients of water-isopropanol mixtures using three experimental techniques: thermogravitational column, optical beam deflection and optical digital interferometry. Lyubimova and Zubova [5] made a numerical study of the onset and the nonlinear regimes of convection in a binary fluid with negative separation ratio. They considered a square cavity heated from above. The study was completed with direct numerical simulations of the nonlinear equations of the problem. They showed that multivortex structures appeared at the onset.

The effect of conducting boundaries on the onset of convection in a binary fluid-saturated porous layer was investigated by Ouattara et al. [6]. The equilibrium solution was found to lose its stability via a stationary bifurcation or a Hopf bifurcation depending on the values of the dimensionless parameters of the problem.

Charrier-Mojtabi et al. [7] presented an analytical and numerical study of the influence of acoustic streaming on species separation in a rectangular cavity filled with a binary fluid mixture under microgravity. They showed that the unicellular flow induced by the Eckart streaming may lead to significant species separation. The analytical results were corroborated by direct numerical simulations using a finite element code (Comsol). In a second part of their study, a linear stability analysis of the unicellular flow was performed using the Galerkin method, a spectral Tau-Chebyshev method, and a finite element method. The results obtained by these three methods were in good agreement.

In addition to the studies on Soret-driven convection, mixed convection in binary mixtures has been the subject of numerous works. Mahidjiba et al. [8] studied the combined action of Soret effect and shear stress on convection both numerically and analytically in a horizontal fluid layer filled with a binary mixture. They showed the existence of subcritical bifurcations for both stabilizing and destabilizing mass flux and the occurrence of multiple steady state solutions for given sets of the control parameters. Kumar et al. [9] studied double diffusive mixed convection in a horizontal channel using velocity–vorticity formulation. They found that the convective heat transfer increased with the thermal Grashof number only with aiding thermo-solutal buoyancy forces. Great attention has been paid to the primary instability corresponding to the onset of double-diffusive mixed convection. Khanafer et al. [10] found that the heat transfer mechanism and the flow characteristics inside a lid-driven cavity were strongly dependent on the Richardson number.

Khouzam et al. [11], in their study of mixed convection in binary mixtures, showed that the mass concentration gradient depended only on two new dimensionless parameters, the mass Rayleigh number,  $Ra_m$ , and the mass Péclet number,  $Pe_m$ , in the case where only the upper horizontal wall was moving. They also demonstrated that species separation was possible for a cell heated from above as well as from below.

Yacine et al. [12] studied the Soret-driven convection and separation of binary mixtures in a horizontal porous cavity subjected to cross heat fluxes. They observed that an increase of the heat flux density ratio led to a decrease in the relaxation time. Recently, Mojtabi et al. [13], carried out an analytical and numerical analysis of the species separation of a binary mixture saturating a porous layer, taking into account the influence of the boundary plates of the cell. They showed that the optimal value of the species separation of the binary mixture did not depend on the thickness or the nature of the walls.

The present study investigates the species separation in a binary fluid mixture, confined in a horizontal rectangular cavity and heated differentially. Two velocities,  $U_p^* \vec{e}_x$  and  $f U_p^* \vec{e}_x$ , are applied at the upper and lower horizontal walls, respectively. The mixed convection ensures better heat and mass transfer rates, as has already been highlighted by previous works considering shear-driven cavities (Khouzam et al. [11] and Bhuvanewari et al. [14]).

An analytical solution is obtained in the case of a shallow cavity. The velocity field obtained is a combination of the flow generated by only the velocity of the walls and the thermoconvective flow under gravity. The mass fraction gradient along the horizontal,  $x$ , axis is then calculated, and the dimensional mass fraction gradient is optimized. The results are corroborated by direct 2D and 3D numerical simulations.

## 2. Mathematical formulation

A horizontal parallelepipedic cell of width  $L$  in the horizontal,  $x$ , direction and height,  $H$ , in the vertical,  $z$ , direction ( $\vec{g} = -g \vec{e}_z$ ), filled with a binary fluid are considered. The cell is subjected to two opposite but constant horizontal velocities at the upper and/or the lower horizontal wall ( $U_p \vec{e}_x, fU_p \vec{e}_x$ ), where  $f$  is a dimensionless constant,  $f \in [-1,1]$  representing the ratio between the two velocities applied at the upper and lower horizontal walls. No-slip conditions are considered on the vertical walls (see Fig.1)

The two horizontal impermeable walls are maintained at different uniform temperatures  $T_1^*$  and  $T_2^*$ , so the cavity can be heated either from above or from below.

It is assumed that the resulting flow is incompressible and the binary Newtonian fluid is modelled as a Boussinesq fluid. Thus, the density of the fluid mixture,  $\rho$ , is a function of the local temperature,  $T^*$ , and the local mass fraction,  $C^*$ . For a small variation of  $T^*$  and  $C^*$  around  $T_0^*$  and  $C_0^*$ , the density varies linearly with local temperature and mass fraction:

$$\rho = \rho_0 [1 - \beta_T (T^* - T_0^*) - \beta_C (C^* - C_0^*)] \quad (1)$$

$\rho_0$  is the fluid mixture reference density at  $T_0^*$  and  $C_0^*$ .

The thermal and mass expansion coefficients ( $\beta_T, \beta_C$ ) are defined as follows:

$\beta_T = -\frac{1}{\rho_0} \left( \frac{\partial \rho}{\partial T^*} \right)_{C^*} > 0$ ,  $\beta_C = -\frac{1}{\rho_0} \left( \frac{\partial \rho}{\partial C^*} \right)_{T^*} < 0$  if  $C^*$  is the mass fraction of the heavier constituent or  $\beta_C < 0$  if  $C^*$  is the mass fraction of the lighter constituent.

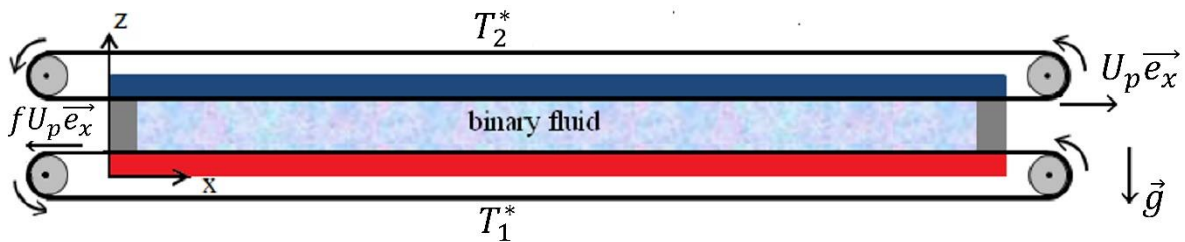


**Fig.1:** Geometry of the physical problem for  $f < 0$

Under these conditions and taking eq. (1) into account, the dimensionless governing equations describing the conservation of mass, momentum, energy and chemical species, in the cavity are written respectively as follows:



$$\left\{ \begin{array}{l} \nabla \cdot \vec{V} = 0 \\ \frac{\partial \vec{V}}{\partial t} + \vec{V} \cdot \nabla \vec{V} = -\nabla P + Ra Pr [T - \psi C] \vec{e}_z + Pr \nabla^2 \vec{V} \\ \frac{\partial T}{\partial t} + \vec{V} \cdot \nabla T = \nabla^2 T \\ \frac{\partial C}{\partial t} + \vec{V} \cdot \nabla C = \frac{1}{Le} (\nabla^2 C + \nabla^2 T) \end{array} \right. \quad (2)$$

The reference scales used are:  $H$  length,  $\frac{H^2}{a}$  for time,  $\rho_0 \frac{a^2}{H^2}$  for pressure, and  $\frac{a}{H}$  for velocity ( $a$  is the thermal diffusivity of the fluid mixture). The dimensionless temperature is given by  $T = \frac{T^* - T_0^*}{\Delta T}$ , where  $\Delta T = T_1^* - T_2^*$ , and  $T_0^* = T_2^*$ . For dimensionless mass fraction, a reference scale based on a non-dimensional combination of the product:

$$\Delta C = \Delta T C_0 (1 - C_0) S_T \text{ is used, where } S_T = \frac{D_T}{D} \text{ is the Soret coefficient.}$$

In 2D, in addition to the aspect ratio,  $A = L/H$ , the problem is governed by six other dimensionless parameters: the thermal Rayleigh number,  $Ra$ , the Prandtl number,  $Pr$ , the Lewis number,  $Le$ , the separation ratio,  $\psi = -\frac{\beta_C D_T}{\beta_T D} C_0 (1 - C_0)$ , the ratio  $f$  between the two velocities of the horizontal plates and the Péclet number,  $Pe$ , which appears in the boundary conditions.

$Ra = \frac{g \beta_T \Delta T H^3}{\nu a}$ ,  $Pr = \frac{\nu}{a}$ ,  $Le = \frac{a}{D}$ ,  $Pe = Pr Re$ , where  $Re = \frac{U_P H}{\nu}$  denotes the Reynolds number.

The 2D mathematical formulation for the boundary conditions is given by:

$$\left\{ \begin{array}{l} z = 1, \vec{V} = Pe \vec{e}_x, T = 0, \frac{\partial C}{\partial z} + \frac{\partial T}{\partial z} = 0, \quad \forall x \in [0, A] \\ z = 0, \vec{V} = f Pe \vec{e}_x, T = 1, \frac{\partial C}{\partial z} + \frac{\partial T}{\partial z} = 0, \quad \forall x \in [0, A] \\ x = 0, A, \vec{V} = 0, \frac{\partial T}{\partial z} = \frac{\partial C}{\partial z} = 0, \quad \forall z \in [0, 1] \end{array} \right. \quad (3)$$

Due to the choice made for the reference temperature  $T_0^*$ , in this study, is equal to  $T_2^*$ , and it follows that, for a cell heated from below, the Rayleigh number is positive, while it is negative for cell heated from above.

### 3. 2D Analytical solution

In the case of a shallow cavity ( $A \gg 1$ ), the governing equations (2) can be considerably simplified, by using the parallel flow approximation, to be solvable analytically

(Mamou et al. [15]). Thus, in the central part of the enclosure, the streamlines are assumed to be parallel to the horizontal walls. In this case, the vertical component of velocity can be neglected:

$$\vec{V}(x, z) = U(z)\vec{e}_x \quad (4)$$

This assumption implies steady-state and leads to the inertia term  $(\vec{V} \cdot \nabla)\vec{V} = \mathbf{0}$  in the Navier – Stokes equation (Eq. (2)). The temperature and mass fraction are written as the sum of a term defining their linear longitudinal variation and a term giving the transverse distribution:

$$T(x, z) = bx + h(z) \quad (5)$$

$$C(x, z) = mx + g(z) \quad (6)$$

where  $b$  and  $m$  are unknown constants representing, respectively, the temperature and mass fraction gradients in the  $x$  direction.  $b = 0$  because of the constant temperatures imposed on the horizontal walls.

Inserting these expressions into equations (2) and after eliminating the pressure in the Navier-Stokes equation, a set of three linear differential equations for the unknowns  $U, T$  and  $C$  is obtained:

$$\begin{cases} \frac{\partial^3 U}{\partial z^3} - Ra \frac{\partial}{\partial x} (T - \psi C) = 0 \\ \nabla^2 T = 0 \\ m Le U - \frac{\partial^2 C}{\partial z^2} = 0 \end{cases} \quad (7)$$

Since the boundary conditions on the vertical walls are not taken into account for the velocity, additional conditions are needed to solve the system of equations (7). They are:

- The mass flow rate through any cross section perpendicular to the  $x$ -axis is equal to zero.
- The mass of the denser component is conserved over the whole cell.

$$\begin{cases} \int_0^1 U dz = 0 \quad \forall x \in [0, A] \\ \int_0^1 \int_0^A C dz dx = 0 \end{cases} \quad (8)$$

By applying these conditions with the boundary conditions (3), the resulting velocity, temperature and mass fraction fields are given by:

$$U = -z(z-1)(2z-1)mRa_m/12Le + ((f+1)z^2 - 2(2f+1)z + f)Pe_m/Le \quad (9)$$

$$T = 1 - z \quad (10)$$

$$C = mx + (2z-1)(6z^4 - 12z^3 + 4z^2 + 2z + 1)Ra_m m^2/1440 + z - (1 + mA)/2 + [(15z^4 - 40z^3 + 30z^2 - 3)f + (15z^4 - 20z^3 + 2)]mPe_m \quad (11)$$

The case where  $f = 0$  (only one velocity is applied, on the upper wall) was studied by Khouzam et al. [14].

To determine the mass fraction gradient,  $m$ , along the  $x$  axis, we require the total mass flux of the component of mass fraction,  $C$ , through any cross section of the rectangular cavity perpendicular to the  $x$  axis, to be equal to zero:

$$\int_0^1 (UC - \frac{1}{Le} (\frac{\partial C}{\partial x} + \frac{\partial T}{\partial x})) dz = 0 \quad \forall x \in [0, A] \quad (12)$$

The latter assumption leads to the following cubic equation giving  $m$  as a function of the dimensionless parameters  $Pe_m$  and  $Ra_m$ .

$$m^3 + 108Pe_m(1-f)m^2/Ra_m - 30240Pe_m(1-f)/Ra_m^2 + ((3456f^2 - 5184f + 3456)Pe_m^2 + 362880 - 504Ra_m)m/Ra_m^2 = 0 \quad (13)$$

where  $Ra_m = (Ra \psi Le)$  is the mass Rayleigh number, and  $Pe_m = (PeLe)$  the mass Péclet number. We deduce that the non-dimensional separation,  $S = mA$ , depends only on  $Pe_m$  and  $Ra_m$  and  $f$ .

## 4. Physical interpretation of analytical results

### 4-1 Velocity field

The intensity of the velocity  $U$  is a function of the three control parameters  $f$ ,  $Pe_m$  and  $Ra_m$

Although the problem studied is a nonlinear one, the velocity field obtained is the superposition of the flow generated only by the velocity of the walls under conditions of weightlessness ( $Pe \neq 0, Ra = 0$ ) and thermoconvective flow under gravity ( $Ra \neq 0, Pe = 0$ ).

One of the objectives of this work is to increase the species separation between the two ends of the cavity ( $x = 0$  and  $x = A$ ). For this, the study will be restricted to  $f \in [-1, 0]$ . For  $f \in [0, 1]$  and moderate values of  $Ra$  and  $Pe$ , the algebraic equation (9) of the second degree in  $z$  admits two real roots on the segment  $z \in [0, 1]$ . The flow obtained in that case consists of two superposed counter-rotating cells leading to weak separation. This is due to the fact that the two convective cells operate in opposite senses. The intensity of the velocity for  $Ra = 0$  and  $Pe = 1$  as a function of  $f \in [0, 1]$  and  $z \in [0, 1]$  is represented in Figure 2.

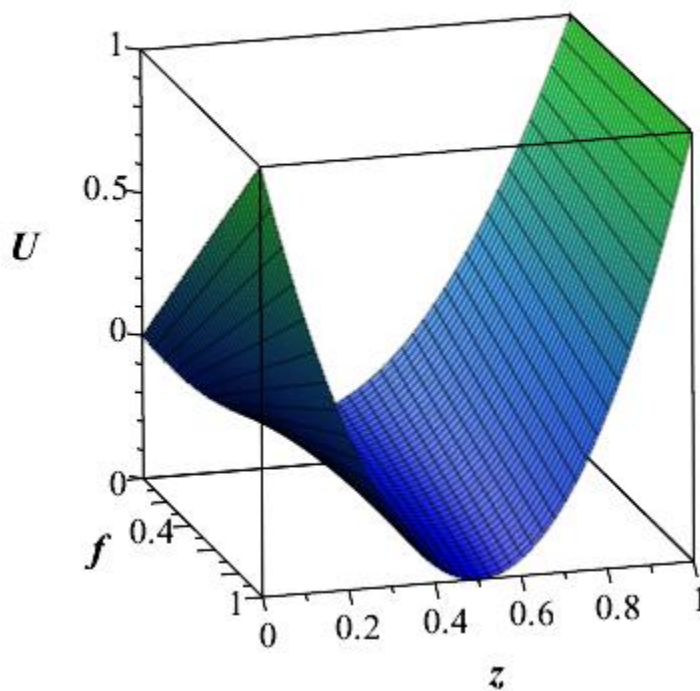


**Fig.2:** Fluid velocity  $U$  as a function of  $f$  and  $z$  for  $Ra=0$  and  $Pe = 1$

It can be observed that the velocity becomes equal to zero at two points over the interval  $z \in [0, 1]$ . Direct numerical simulations confirm the analytical results found in Figure 9.a and 9.b showing the two superimposed rolls along the  $x$  axis.

In the case where  $Pe$  and  $Ra$  are not equal to zero and  $f \in [-1, 0]$ , the algebraic equation (9) of the third degree in  $z$  admits a single real root  $z_0 \in [0, 1]$ . It follows that the flows generated in the cavity are unicellular. It is easy to check that for:

$Pe_m = 0, Ra_m \neq 0, z_0=1/2$  and for  $Pe_m \neq 0, Ra_m = 0$  equation (9) admits two roots:  
 $z_{01} = (2f + 1 + \sqrt{f^2 + f + 1})/3(f + 1)$  and  $z_{02} = (2f + 1 - \sqrt{f^2 + f + 1})/3(f + 1)$ ,  
 only the root  $z_{01}$  verifies  $z_{01} \in [0, 1]$ .

The velocity field (9) can be written as:

$$U_{uni} = p(z) Ra_m \psi + q(z, f) Pe$$

where  $p(z) = -z(z - 1)(2z - 1)/12$  and  $q(z, f) = (f + 1)z^2 - 2(2f + 1)z$ .

According to equation (13), the mass fraction gradient is a function of  $Ra_m, Pe_m$ , and  $f$ :

$m = n(Ra_m, Pe_m, f)$ . The mass Rayleigh number is equal to:  $Ra_m = Ra \psi Le = Kg\Delta TH^3$  where  $K$  depends only on the binary mixture. The thickness,  $H$ , is also fixed when the cavity is made. Under these conditions, the mass fraction gradient depends on the product  $g\Delta T$ ,  $Pe_m = U_p^* H/D$ . It is possible experimentally to vary the product  $g\Delta T$ , the velocity  $U_p^*$  and the coefficient  $f$  independently.

The objective being to obtain the species separation of the mixture,  $\Delta T$  must be different from zero. When the intensity of gravity,  $g$ , tends to zero,  $Ra$  tends to 0, the situation found in microgravity. It follows that the velocity  $U_{uni}$  tends to  $q(z, f) Pe$ . The mass fraction gradient  $m$  depends only on  $Pe$  and  $f$ , once the temperature difference  $\Delta T$  and the thickness  $H$  of the cavity and the binary mixture have been fixed.

When the velocity of the horizontal plates  $U_p^*$  tends to zero, the Péclet number tends to 0. The intensity of the fluid velocity  $U_{uni}$  is proportional to the product  $Ra \psi m$ . The mass fraction gradient, in this case ( $Pe = 0$ ), is a function of  $Ra_m$  only and does not depend on  $f$ . For  $Pe = 0$ , equation (13) has three solutions:

$$m = 0 \text{ and } m = \pm 6\sqrt{14Ra_m - 10080}/Ra_m \quad (14)$$

The solution  $m = 0$  corresponds to the absence of movement and consequently of separation, and the other two solutions are real solutions only if the mass Rayleigh number verifies:

$$Ra_m = \psi Le Ra > \frac{10080}{14} = 720 = \psi Le Ra_c \quad (15)$$

where  $Ra_c$  is the the linear critical thermal Rayleigh number leading to the onset of unicellular flow, a result previously obtained by Knobloch et al. [16].

The separation factor,  $\psi$ , has the same sign as the thermodiffusion coefficient,  $D_T$ , if  $\beta_c < 0$ .

In that case:

-for  $\psi > 0$ , species separation is possible only for bottom heating ( $Ra > 0$ ), if  $Ra > 720/\psi Le$ .

-for  $\psi < 0$ , the species separation is possible only for top heating ( $Ra < 0$ ) if  $Ra < 720/\psi Le$ .

For a cell heated from below,  $Ra > 0$ , the heavier component migrates towards to the top cold wall since  $\psi > 0$ . For  $\psi < 0$  and  $Ra < 0$ , in a cell heated from above, the heavier component migrates towards the top hot wall. In these two configurations, the heaviest component migrates towards the top wall.

For  $Pe_m \neq 0$ , system of equations (17) has 4 roots, two real opposite and two complex conjugates.

The ratio of the optimal values  $m^*_{opt2}(f=-1)/m^*_{opt2}(f=0)$  as a function of  $\Delta T$  and  $H$  is presented in figure 3. It shows that  $m^*_{opt2}$  for  $f=-1 > m^*_{opt2}$  for  $f=0 \forall H \in [0.5 \text{ mm}, 4 \text{ mm}]$  and  $\Delta T \in [-40^\circ \text{ C}, 40^\circ \text{ C}]$  and especially for the negative values of the temperature difference  $\Delta T$  imposed on the cavity.

Kouzam et al. [11], obtained  $m_{opt2} = 0.432$  for  $Pe_m = 6.5$ . In this paper, for the same value of  $Pe_m = 6.5$ ,  $m_{opt2} = 0.462$  for  $f = -1$ . Thus, the species separation increases around 7%.

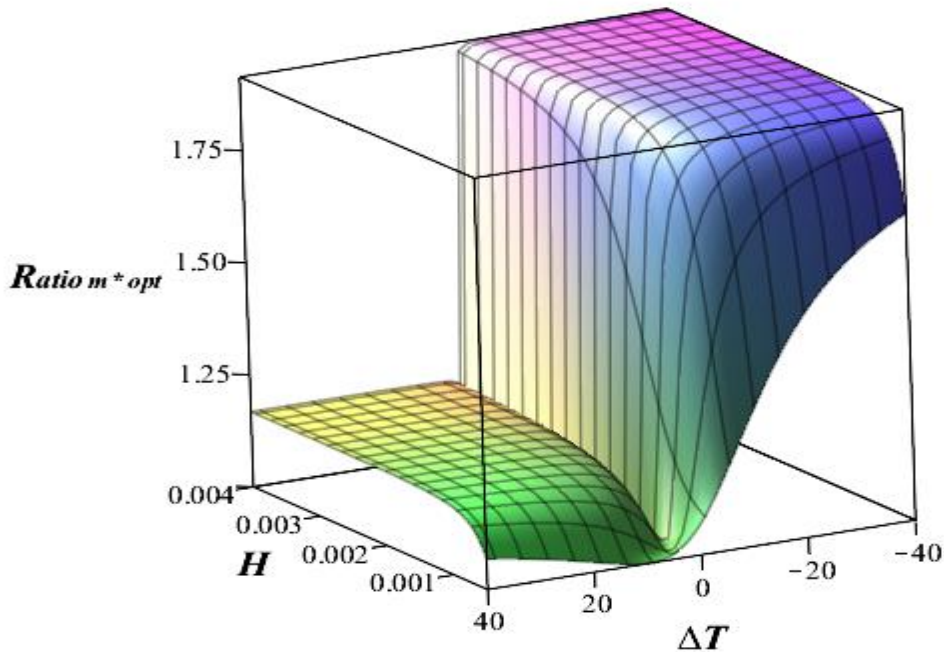


**Fig.3:** Ratio of the optimal values  $m^*_{opt2}(f=-1)/m^*_{opt2}(f=0)$  as a function of  $\Delta T$  and  $H$

## 4.2 The dimensional species separation

The non-dimensional species separation,  $S = m A$ , is defined as the product of the non-dimensional mass fraction gradient,  $m$ , along the x-axis, by the aspect ratio,  $A$ , of the cavity. It characterizes the difference between the mass fraction of the heaviest constituent in the vicinity of the two vertical walls of the horizontal cavity. The mass fraction  $C^*$  has been replaced by:  $(C^* - C_0^*)/\Delta C$  where  $\Delta C = \Delta T C_0(1 - C_0)S_T$ , which represents a non-dimensional reference scale.

It is no longer possible to calculate the effective optimum mass separation  $S^*$  without returning to the dimensional formulation of the problem.

The effective mass separation between the two vertical ends ( $x = 0$ ) and ( $x = L$ ) of the cavity is given by

$$S^* = m^*L = \frac{\partial C^*}{\partial x^*}L = \Delta T C_0 (1 - C_0) D_T \left(\frac{\partial C}{\partial x}\right)L/DH = E (\Delta T/H) mL \quad (16)$$

where  $E = C_0(1 - C_0) D_T/D$  is a fixed constant characteristic of the binary solution studied.

For non-zero  $Ra_m$  and  $Pe_m$ , equation (13) has one real root and two complex conjugate roots. The real solution  $m^*$  is obtained by replacing  $m$ ,  $Ra_m$  and  $Pe_m$  by their respective expressions as functions of  $\Delta T$  and  $H$  in equation (13),  $Ra_m = Ra \psi Le = -Kg\Delta TH^3$ , where  $K = \beta_C C_0(1 - C_0) D_T/\nu D^2 = \beta_C E / \nu D$

The optimal value of the effective horizontal mass fraction gradient,  $m_{opt}^*$ , depends on the physical parameters  $\Delta T, H, U_p^*$  and  $f$ , where  $U_p^*$  is the dimensional velocity of the horizontal plates. The value,  $H$ , of the thickness of the cavity is fixed when the experimental cell is manufactured. The optimum of  $m^*$  depends on the three control parameters,  $\Delta T, U_p^*$  and  $f$ . The values  $\Delta T$  and  $H$  are left open initially and the partial optimization of the horizontal mass gradient noted by  $m_{opt}^*$  will be based on parameters  $U_p^*$  and  $f$ . For this, the following system of equations is solved:

$$\begin{cases} \partial m^* / \partial U_p^* = 0 \\ \partial m^* / \partial f = 0 \\ \text{modified, Eq. (13)} \end{cases} \quad (17)$$

where the modified equation (13) corresponds to equation (13) with  $m$  replaced by its expression:  $m = (H/E \Delta T)m^*$ . The resolution of the algebraic system (17) leads to all of the following solutions, given the values of  $U_{opt}^*$ ,  $f_{opt}$  and the associated value of  $m_{opt}^*$ :

$$\left\{ \begin{array}{l} U_{opt1}^* = 0 \\ m_{opt1}^* = \pm \nu D \sqrt{504gK\Delta TH^{*3} - 362880} / g\beta_c H^{*4} \end{array} \right. \quad (18)$$

This mass fraction gradient can also be written in the form:

$$m_{opt1}^* = \pm \frac{\sqrt{504C_0(1-C_0)\nu g D_T |\beta_c| \Delta T H^3 - 36288\nu^2 D^2}}{g\beta_c H^4} \quad (19)$$

This first optimum  $m_{opt1}^*$ , with respect to  $U_p^*$  and  $f$  obtained for  $U_{opt1}^* = 0$ , corresponds to the solution already found previously in equation (13), when  $Pe = 0$ .

The second optimum  $m_{opt2}^*$  is given by:

$$\left\{ \begin{array}{l} f_{opt} = -1 \\ U_{opt2}^* = \pm F(\Delta T, H, K, g) \\ m_{opt2}^* = \pm 2\nu D \frac{\sqrt{-126gK\Delta TH^3 + 84\sqrt{21g^2K^2\Delta T^2H^6 + 45360gK\Delta TH^3 + 228614400 - 1270080}}}{g\beta_c H^4} \end{array} \right. \quad (20)$$

where the expression of the function  $F$  is not specified because of its great length.

To illustrate our study, we chose the water-ethanol binary mixture previously studied by Platten et al. [17]. The values of the thermophysical properties of this binary solution, at the average temperature  $T = 22.5 \text{ }^\circ\text{C}$ , are given in Table 1.

Table 1: Properties for a water (60.88 wt%) - ethanol (39.12 wt%) mixture at a mean temperature of  $22 \text{ }^\circ\text{C}$ .

Property	Value
$\alpha [m^2s^{-1}]$	$10^{-7}$
$D [m^2s^{-1}]$	$4.32 \cdot 10^{-10}$
$D_T [m^2s^{-1}K^{-1}]$	$1.37 \cdot 10^{-12}$



$\beta_c$	-0.212
$\beta_T$ [1/K]	$7.86 \cdot 10^{-4}$
$\nu$ [ $m^2s^{-1}$ ]	$2.716 \cdot 10^{-6}$
$\rho_0$ [ $kgm^{-3}$ ]	935.17

The associated Prandtl number, Lewis number and separation ratio for this water-ethanol binary mixture are  $Pr = 27.15$ ,  $Le = 232.15$  and  $\psi = 0.2$ .

The expressions of  $m_{opt1}^*$  and  $m_{opt2}^*$  do not admit an optimum with respect to  $\Delta T$  and  $H$ . On the other hand, these gradients admit an optimum with respect to  $H$  for fixed  $\Delta T$  or with respect to  $\Delta T$  for fixed  $H$ .

Equation (19), for fixed  $\Delta T$ , allows us to determine the thickness ensuring the maximum species separation  $m_{opt1}^*$ :

$$H_{opt1} = \left( \frac{72\nu D^2}{C_0(C_0-1)gD_T\beta_C\Delta T} \right)^{1/3} \quad (21)$$

For the binary mixture considered and for  $\Delta T = 10^\circ C$  we obtain  $H_{opt1} = 1.75 \cdot 10^{-4}m$ .

The evolution of  $m_{opt1}^*$  as a function of  $H$  for  $\Delta T = 10^\circ C$  is shown in Figure 4.

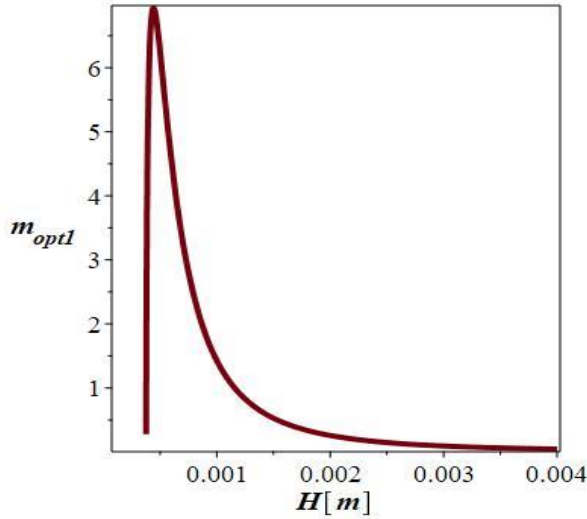


**Fig. 4:** Effective mass fraction gradient  $m_{opt1}^*$  as a function of  $H$  at  $\Delta T = 10^\circ C$  for the binary mixture water (60.88 wt%)- ethanol,  $\psi = 0.2$  and for  $Pe_m = 0$ .

The evolution of  $m_{opt1}^*$  as a function of  $H \in [10^{-3}m, 4 \cdot 10^{-3}m]$  and  $\Delta T \in [10^\circ C, 80^\circ C]$  is shown in figure 5.

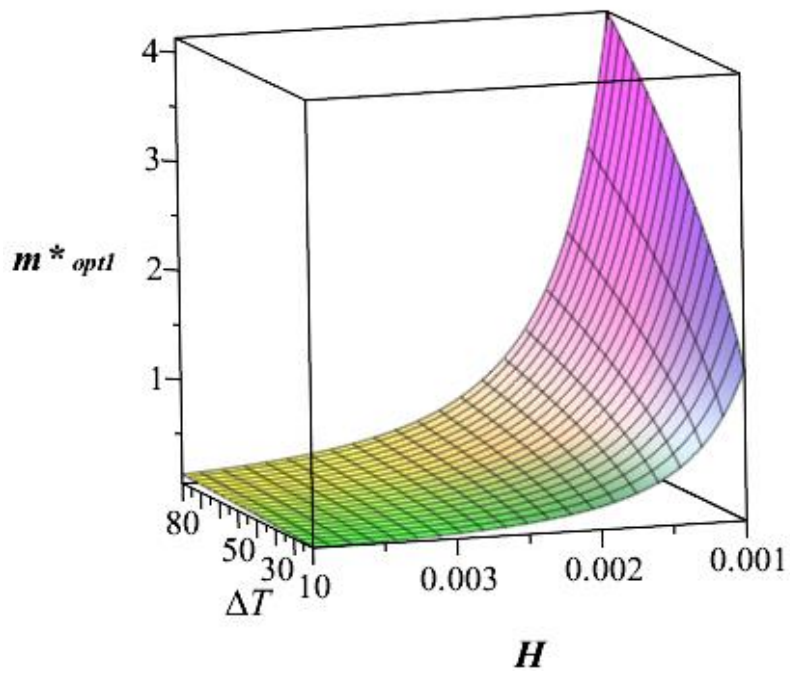


**Fig. 5:** Effective mass fraction gradient  $m^*_{opt1}$  as a function of  $H$  and  $\Delta T$  for the water-ethanol binary mixture,  $\psi = 0.2$  ( $Pe_m = 0$ ).

For  $Ra \neq 0$  and  $Pe \neq 0$ :

- the evolution of the optimum velocity  $U^*_{opt2}$  with  $H \in [10^{-3}m, 4.10^{-3}m]$  and  $\Delta T \in [10^\circ C, 80^\circ C]$  is shown in figure 6.

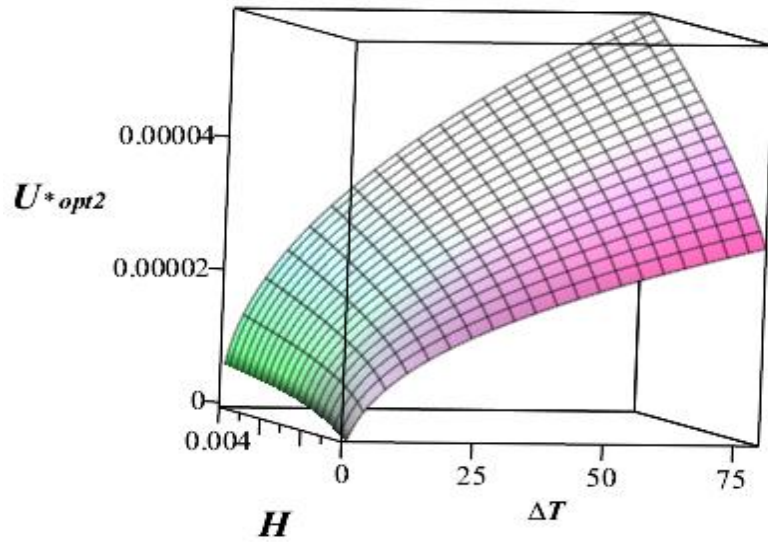


**Fig. 6:** Velocity  $U^{*opt2}$  as a function of  $H$  and  $\Delta T$  for the water-ethanol binary mixture,  $\psi = 0.2$

- the evolution of the optimum mass fraction gradient  $m^{*opt2}$  with  $H \in [10^{-3}m, 4.10^{-3}m]$  and  $\Delta T \in [10^\circ C, 80^\circ C]$  is shown in Figure 7.

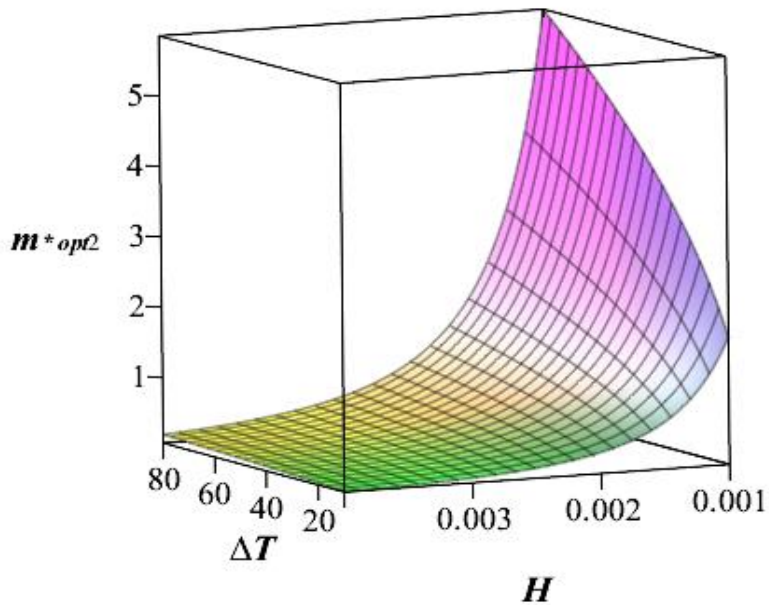


**Fig.7:** Optimal effective mass fraction gradient  $m^{*opt2}$  as function of  $H$  and  $\Delta T$  for the water-ethanol binary mixture,  $\psi = 0.2$

- the evolution of the optimum mass fraction gradient  $m^{*opt2}$  with

$H \in [10^{-3}m, 4.10^{-3}m]$  and  $\Delta T \in [-80 \text{ } ^\circ C, -10 \text{ } ^\circ C]$ , cell heated from the top is shown in Figure 8.

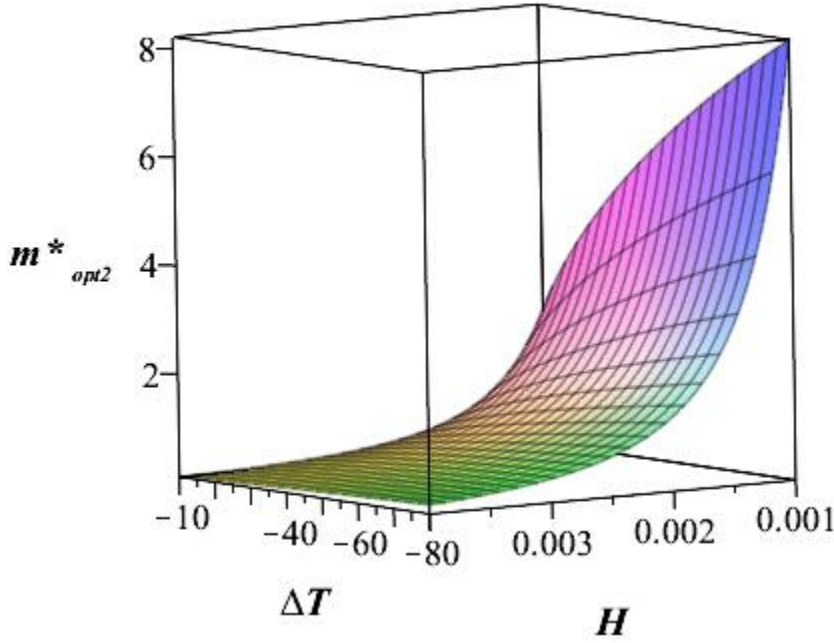


**Fig.8 :** The optimal mass fraction gradient  $m_{opt2}^*$  as a function of  $H$  for  $\Delta T \in [-80 \text{ } ^\circ C, -10 \text{ } ^\circ C]$  for the water-ethanol binary mixture,  $\psi = 0.2$ .

It can be seen that, in the case of a cell heated from above,  $\Delta T \in [-80 \text{ } ^\circ C, -10 \text{ } ^\circ C]$  and  $\psi > 0$ , the fluid layer is stable regardless of the thermal Rayleigh number imposed. The flow is induced only by the velocity imposed on the horizontal walls. The fluid layer is subjected to forced convection. That is why, to increase the value of  $m_{opt2}^*$ , it is sufficient to maintain the layer at the largest temperature difference compatible with the binary fluid studied.

On the other hand, for a cell heated from below with  $\psi = 0.2$  and  $Pe \neq 0$ , even for small temperature differences ( $\Delta T = 4 \text{ } ^\circ C$ ) and small thicknesses ( $H = 3.10^{-3}m$ ), the thermal Rayleigh number is equal to  $Ra = 30.66$ . This thermal Rayleigh number is higher than the critical Rayleigh number,  $Ra_c = 720/\psi Le = 15.55$ , associated with the onset of the unicellular thermal convection. This thermal convection is added to the forced convection motion induced by the velocity imposed on the walls of the cavity.

An analysis of Figures 4, 6 and 7, shows that for fixed  $\Delta T$ ,  $m_{opt2}^*$  increases when  $H$  decreases and, for a fixed  $H$ ,  $m_{opt2}^*$  increases when  $|\Delta T|$  increases. The velocity  $U_{p2}^*$  also

depends on  $\Delta T$  and  $H$ . The objective of this study being to obtain the optimal separation, the values of  $\Delta T$  and  $H$  chosen for  $m_{\text{opt}2}^*$  will be taken for the  $U_{P_2}^*$  calculation.

## 5. Direct numerical simulation

### a- 2.D Direct numerical simulations

The dimensionless system of equations (2) associated with the boundary conditions (3) was solved numerically using a finite element code (Comsol Multiphysics). The rectangular mesh was preferred to the triangular mesh because the cavity studied was rectangular. After verifying that, for an aspect ratio of the cavity greater than 6, the vertical walls have very little influence on the flow and transfers in the central part of the cavity, the authors decided to consider a cavity with an aspect ratio of 10 throughout the rest of the study. The quadrangle spatial resolution is 30-150 or 40-200 and the results obtained with these two meshes are similar even for large values of  $Ra$  and  $Pe$  numbers.

In the case of  $f \in [0, 1]$  and for  $Pe = 0.6$ , the velocity fields obtained using direct numerical simulations for  $Ra = 0$  ( $g = 0, \Delta T \neq 0$ ) and  $Ra = 100$  are identical and correspond to the analytical results exactly (Fig. 9a). For low values of  $Ra$ , the binary fluid layer is in a pure heat conduction state and the fluid is moved only by the horizontal walls. The numerical and analytical results also show that the temperature field verifies the equation:  $T = 1 - z$ .

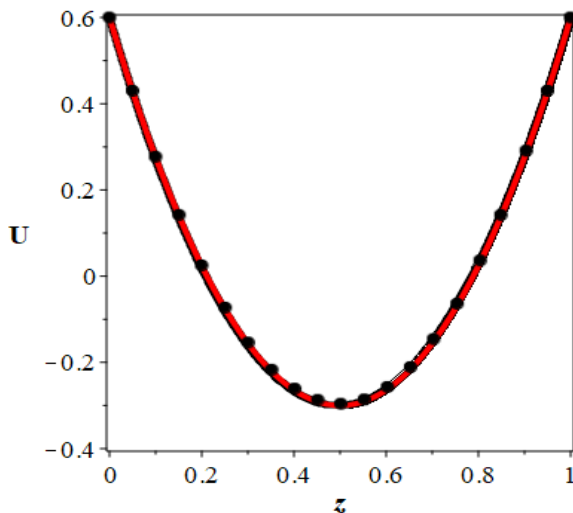


**Fig.9a:** Velocity,  $U(z)$  for  $f = 1$ ,  $Pe = 0.6$ , for  $Ra = 0$  and  $Ra=100$ , obtained analytically (continuous line) and using direct numerical simulation (dotted line).

Fig. 9b, obtained for the same values of the parameters of the water-ethanol binary mixture, shows that the structure of the flow is formed by two counter-rotating rolls. The mass fraction gradients induced by the rotation of each of these cells are opposite. It follows that for  $z \in [0, 1/2]$  the mass fraction field increases between  $x = 0$  and  $x = A$ , and the opposite is true for  $z \in [1/2, 1]$  as indicated by the surface colour.

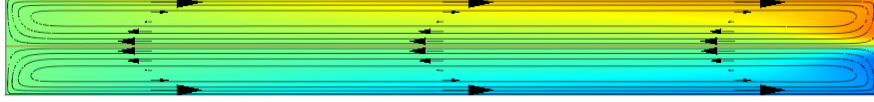


**Fig.9b:** Stream function (continuous lines) and mass fraction field (in colour) for  $f = 1$ ,  $Ra = 100$ ,  $Pe = 0.6$

For the unicellular flow obtained for  $f = -1$ , in order to evaluate the mass fraction gradient along the horizontal axis,  $C(x)$  was plotted along the axis  $z = \frac{1}{2}$  between  $x = 0$  and  $x = A$  and the slope of this curve was determined between  $x = 2$  and  $x = 8$ , in order to eliminate the effects of recirculation in the vicinity of the vertical ends. The results, obtained by solving the full governing equations (2) with the boundary conditions (3), are in good agreement with the analytical solution based on the parallel flow approximation.

Two cases were considered: the case with no velocity applied to the walls,  $U_p = 0$ , and the case of two velocities applied ( $f = -1$ ), to the upper wall and the lower one with  $U_p$  corresponding to the optimal velocity in accordance with  $m_{opt2}^*$ . For  $U_p = 0$  and for water-ethanol binary mixture ( $\psi > 0$ ), the heavier component (water) moves towards the cold wall. If  $Ra < 0$ , in a cell heated from above, the fluid layer is in stable mechanical equilibrium and thermogravitational separation is not possible. It is only possible when the cell is heated from below,  $Ra > 0$  and  $\psi > 0$ ,  $m_{opt1}^* = 0.448 m^{-1}$ . For  $U_p \neq 0$ ,  $f = -1$ , the separation is possible whether the cell is heated from below or from above ( $Ra > 0$  and  $Ra < 0$ ).

For a cavity of fixed thickness  $H_2 = 2 \cdot 10^{-3} m$ , and a temperature difference  $\Delta T = 5$ , the associated Péclet and Rayleigh numbers for water-ethanol binary mixture are  $Pe = 0.198$  and  $Ra = 1125.6$ . The mass fraction gradient is equal to  $m_{opt2}^* = 0.0639 m^{-1}$  and the associated dimensional velocity  $U_{opt2}^* = 9.931 \cdot 10^{-6} m \cdot s^{-1}$ . This result is in good agreement with the direct simulation results obtained, cf. Fig.10.

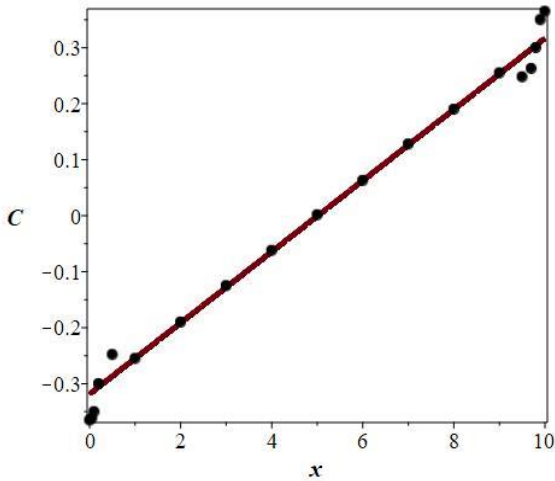


**Fig.10:** The water-ethanol binary mass fraction  $C(x)$ , for  $f = -1$ ,  $Ra = 1135.6$ ,  $Pe = 0.198$ , obtained analytically (continuous line) and using direct numerical simulation (dots).

For values of  $\Delta T < 0$ ,  $Ra < 0$  and  $\psi > 0$ , as is the case of water(60,88%)-ethanol(39,12%) binary mixture, the flow is only induced by the forced convection due to the wall velocities,  $\pm U_p$ . In this case, to increase the phenomenon of thermodiffusion between the vertical walls, it is necessary to increase the temperature difference  $|\Delta T|$ . The optimum species separation of the binary mixture is obtained once the optimal velocity  $U_{p2}$  has been calculated, for a given choice of  $H$  and  $|\Delta T|$ . For  $H_2 = 2 \cdot 10^{-3}m$  and  $|\Delta T| = 50$ , the maximum species separation obtained for the water ethanol binary mixture is  $m_{opt2}^* = 0.8989 m^{-1}$  and the associated velocity  $U_{opt2}^* = 5.597 \cdot 10^{-5}m/s$

Equation (13) shows that the adimensional mass fraction gradient,  $m$ , is a function of the two dimensionless numbers  $Ra_m$  and  $Pe_m$ . The evolution of the species separation between the two ends of the cavity, expressed by  $S = mA$ , is shown in Figure 9 for  $Pe_m = 0$  ( $U_2=0$ ) and for  $Pe_m = 14.5$  for water-Ethanol. For  $Pe_m = 0$ , the separation is only possible when the cell is heated from below ( $Ra_m > 0 \Rightarrow Ra > 0$ ) since  $\psi > 0$ . For the second case,  $Pe_m = 14.5$ , the species separation is possible even if the cell is heated from below or from above (positive or negative value of  $Ra$ ). The analytical result (continuous line) is in good agreement with the numerical results represented by the dots. The colour scales associated with 4 points in Fig.11 indicate the water mass fraction in the cavity and the curves in black represent the separation  $S = mA$ .

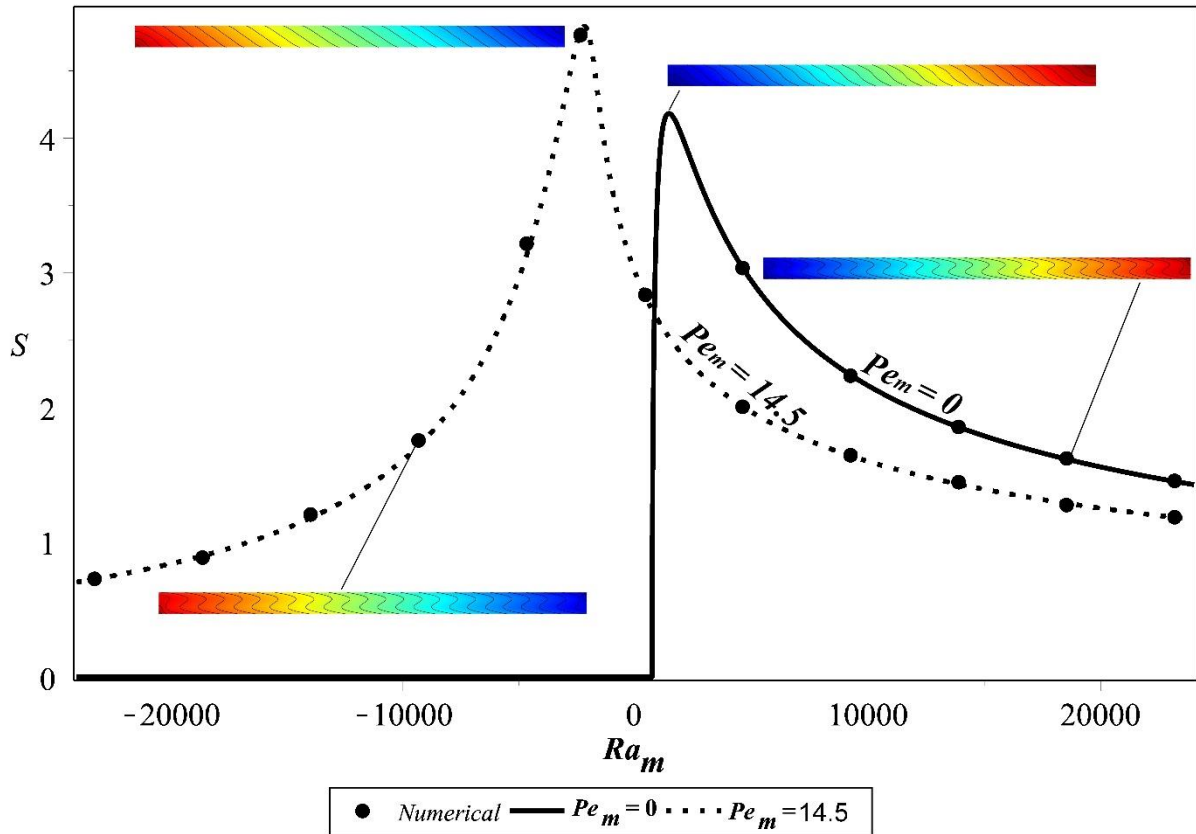


**Fig.11:** Separation value versus the mass Rayleigh number for  $Pe_m = 0$  and  $Pe_m = 0, 14.5$

From a binary mixture of uniform mass fraction, the time  $\tau$  needed to achieve such separation was at least as important as the separation level. The relaxation time of the separation process was analysed numerically for two values of Péclet number,  $Pe_m = 2$  and  $Pe_m = 14.5$ . Fig. 12 shows the temporal evolution of the mass fraction of the denser component (water) with  $Ra_m = 700$  and  $f = -1$ . The steady state can be reached considerably faster with high values of  $Pe_m$ , which correspond to a higher velocity imposed on the horizontal walls of the cavity. The ratio of mass Péclet numbers is equal to the ratio of the associated velocities:

$14.5/2 = U_{p2}/U_{p1}$ . It can be seen that the relaxation time decreases as the speed of the walls increases, which leads to a decrease in the separation of the species.



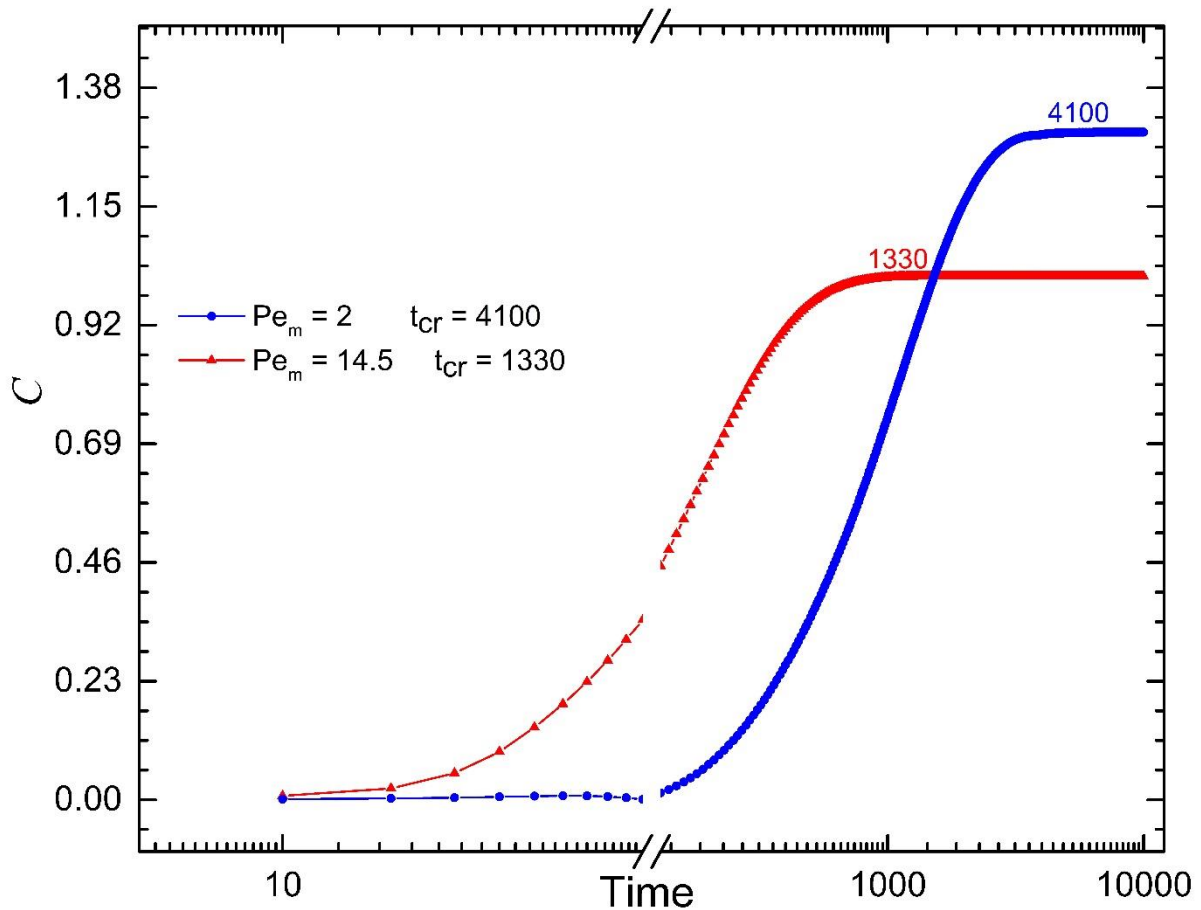
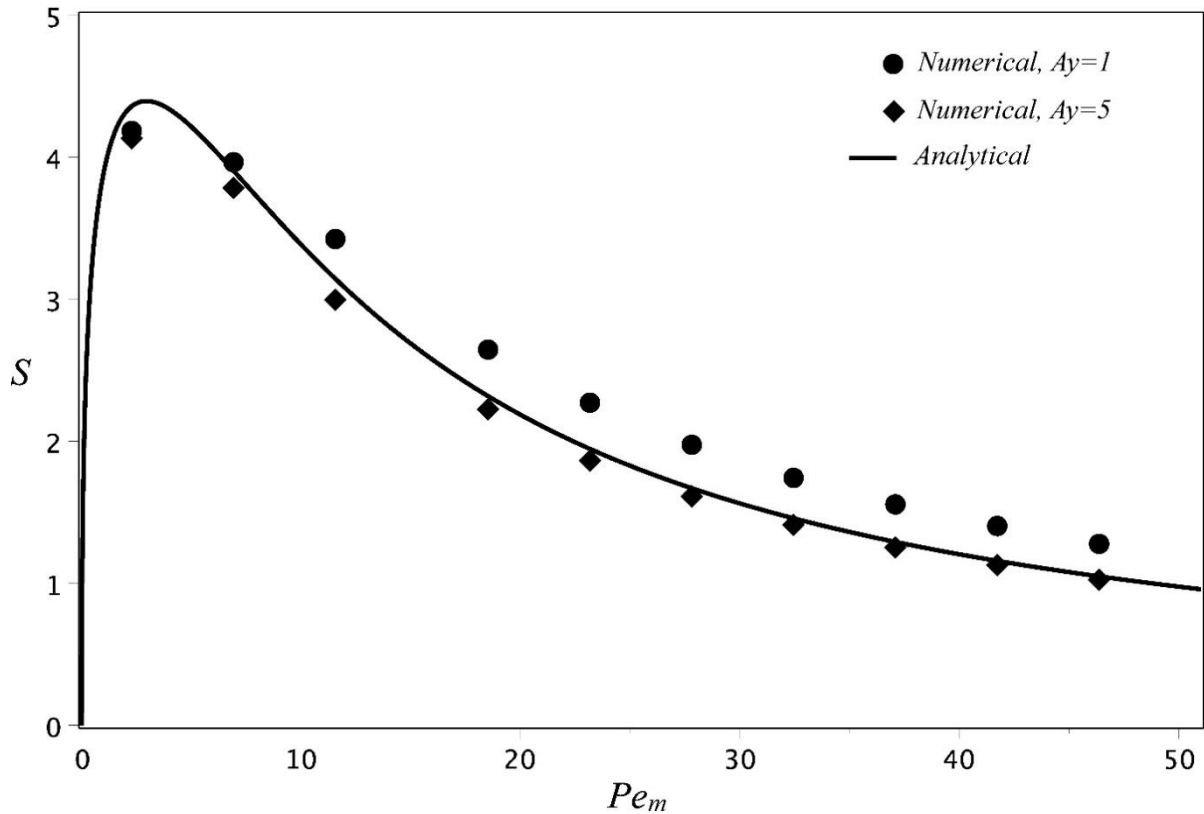


Fig.12 Mass fraction  $C(t, x=8, y=0.7)$  for  $Ra_m = 700$ ,  $f = -1$  and for two values of  $Pe_m$

### b-Comparison between 2D and 3D direct numerical simulations

3D numerical simulations were carried out for  $f = -1$  in a parallelepipedic cavity of aspect ratio  $A = L/H = 10$  along the x axis, as in 2D, and aspect ratios according to the third direction  $Ay = 1$  and  $Ay = 5$  respectively. The analytical values of the non-dimensional species separation  $S = mA$  as a function of  $Pe_m$ , for  $Ra_m = 700$  and for  $f = -1$  and those calculated from 3D direct numerical simulations in the vertical median planes  $y = 1/2$  and  $y = 5/2$  are shown in Fig.13. For  $Ay = 1$ , the median plane  $y = 1/2$  is too close to the planes  $y = 0$  and  $y = 1$ , which explains the better agreement between the analytical results obtained for an infinite horizontal extension cavity and the 3D results for the cavity with aspect ratio  $Ay = 5$ .



**Fig.13:** Separation as a function of mass Péclet number for  $A_y = 1$  and  $A_y = 5$  for  $Ra_m = 700$  and  $f = -1$ .

## 6. CONCLUSION

Analytical and numerical studies were performed to investigate the species separation in a horizontal rectangular (or parallelepipedic) cavity filled with a binary fluid heated from below or from above. Constant velocity was imposed on the top and/or the bottom plate of the cavity. The analytical solution was determined using the parallel-flow assumption. The velocity obtained corresponds to the superposition of the velocity in the presence of natural convection alone ( $Pe = 0$ ) and forced convection ( $Ra = 0$ ) velocity induced by the velocities imposed on the horizontal walls.

The non-dimensional formulation showed that the non-dimensional species separation,  $S$  depends only on three dimensionless parameters: the mass Rayleigh number and the mass Péclet number and the velocity ratio  $f$ . Dimensional separation,  $S^*$  depends on four parameters:

$f, U_p, \Delta T, H$  and the thermophysical characteristics of the water-ethanol mixture mentioned in Table 1.

For  $f \in [0,1]$  and for low values of  $U_p$ , the flow obtained consists of 2 superimposed counter-rotating cells leading to a very weak species separation. For  $f \in [-1,0]$ , the optimization according to the 4 parameters  $f, U_p, \Delta T$  and  $H$ , on which the separation depends, shows that this problem admits an optimum with respect to the first two parameters only ( $f, U_p$ ). This partial optimum is obtained when the two horizontal walls are moving at equal speed but in opposite directions,  $f = -1$ . The intensity of the  $U_2^*$  velocity of the walls is obtained as a function of  $\Delta T$  and  $H$ , and is of the order of  $10^{-5} \text{ m/s}$  for the water-ethanol mixture studied and for a cavity of thickness  $H = 2.10^{-3} \text{ m}$ .

The time needed to obtain the separation starting from a homogeneous binary solution decreases as the mass Péclet number increases. However large values of Péclet number decrease the species separation. Therefore, there is a compromise to be found between the separation intensity and the time needed for the separation. The direct, 2D and 3D, numerical simulations were performed and confirmed the validity of the analytical results.

**Acknowledgements:** The authors are grateful to CNES (Centre National d'Etudes Spatiales) for its financial

## References

- [1] A. M. Al-Amiri, K. M. Khanafer, and I. Pop, Numerical Simulation of Combined Thermal and Mass Transport in a Square Lid-Driven Cavity, *Int. J. Therm. Sci.*, vol. 46, pp. 662–671, (2007).
- [2] J. Koseff. The lid-driven cavity flow: a synthesis of qualitative and quantitative observations. *Journal of Fluids Engineering*. vol. 106. pp. 390-398. (1984).
- [3] M. C. Charrier-Mojtabi. B. Elhajjar. and A. Mojtabi. Analytical and numerical stability analysis of Soret-driven convection in a horizontal porous layer. *Physics of Fluids*. vol. 19. (2007).
- [4] A. Mialdun. A. Yasnou. V. Shetsova.. W. Köhler. MM. Bou-Ali. A comprehensive study of diffusion. thermodiffusion. and Soret coefficients of water-isopropanol mixtures. *J. Chem Phys*. 136:244512 (2012).
- [5] T. Lyubimova. N. Zubova Onset and nonlinear regimes of convection of binary fluid with negative separation ratio in square cavity heated from above. *International Journal of Heat and Mass Transfer*. vol. 106. pp. 1134–1143. (2017).
- [6] B. Ouattara. A. Khouzam. A. Mojtabi. and M. C. Charrier-Mojtabi. Analytical and numerical stability analysis of Soret-driven convection in a horizontal porous layer: the effect of conducting bounding plates. *Fluid Dynamics Research*. vol. 44. Jun (2012)
- [7] M. C. Charrier-Mojtabi. A. Fontaine. and A. Mojtabi. Influence of acoustic streaming on thermo-diffusion in a binary mixture under microgravity. *International Journal of Heat and Mass Transfer*. vol. 55. pp. 5992-5999. Oct. (2012).

- [8] A. Mahidjiba, R. Bennacer, and P. Vasseur. Flows in a fluid layer induced by the combined action of a shear stress and the Soret effect. *International Journal of Heat and Mass Transfer*. vol. 49. pp. 1403-1411. Apr. (2006).
- [9] D. S. Kumar, K. Murugesan, and A. Gupta. Effect of thermo-solutal stratification on recirculation flow patterns in a backward-facing step channel flow. *International Journal for Numerical Methods in Fluids*. vol. 64. pp. 163-186. Sep. (2010).
- [10] K. Khanafer and K. Vafai. Double-diffusive mixed convection in a lid-driven enclosure filled with a fluid-saturated porous medium. *Numerical Heat Transfer Part a-Applications*. vol. 42. pp. 465-486. Oct. (2002).
- [11] A. Khouzam, A. Mojtabi, M.-C. Charrier-Mojtabi, and B. Ouattara. Species separation of a binary mixture in the presence of mixed convection. *International Journal of Thermal Sciences*. vol. 73. pp. 18-27. 11. (2013).
- [12] L. Yacine, A. Mojtabi, R. Bennacer, and A. Khouzam. Soret-driven convection and separation of binary mixtures in a horizontal porous cavity submitted to cross heat fluxes. vol. 104. pp. 29-38. (2016).
- [13] A. Mojtabi, B. Ouattara, D. A. S. Rees, M.C. Charrier-Mojtabi, The effect of conducting bounding horizontal plates on species separation in porous cavity saturated by a binary mixture. *International Journal of Heat and Mass Transfer*, 126, pp. 479-488 May (2018)
- [14] M. Bhuvaneshwari, S. Sivasankaran, and Y. J. Kim. Numerical study on double diffusive mixed convection with a Soret effect in a two-sided lid-driven cavity. *Numerical Heat Transfer Part a-Applications*. vol. 59. pp. 543-560. (2011).
- [15] M. Mamou, P. Vasseur, and E. Bilgen. Analytical and numerical study of double diffusive convection in a vertical enclosure. *Heat and Mass Transfer*. vol. 32. Issue1/2, pp. 115-125. Nov. (1996)
- [16] E. Knobloch and D. R. Moore. Linear stability of experimental Soret convection. *Phys. Rev. A* 37(3):670-680. Feb. (1988).
- [17] J.K. Platten, M.M. Bou-Ali, J.F. Dutrieux. Enhanced molecular separation in inclined thermogravitational columns. *J. Phys. Chem. B* 107 (42) .11763-11767 (2003).